Stochastic Bias from Non-Gaussian Initial Conditions

Daniel Baumann[★], Simone Ferraro[♢], Daniel Green[♣,♦,♠], and Kendrick M. Smith[♢,♡]

[★] *D.A.M.T.P., Cambridge University, Cambridge, CB3 0WA, UK*

[♢] *Princeton University Observatory, Peyton Hall, Ivy Lane, Princeton, NJ 08544, USA*

[♣] *School of Natural Sciences, Institute for Advanced Study, Princeton, NJ 08540, USA*

[♦] *Stanford Institute for Theoretical Physics, Stanford University, Stanford, CA 94306, USA*

[♠] *Kavli Institute for Particle Astrophysics and Cosmology, Stanford, CA 94025, USA*

[♡] *Perimeter Institute for Theoretical Physics, Waterloo, ON N2L 2Y5, Canada*

Abstract

In this article, we show that a stochastic form of scale-dependent halo bias arises in multi-source inflationary models, where multiple fields determine the initial curvature perturbation. We derive this effect for general non-Gaussian initial conditions and study various examples, such as curvaton models and quasi-single field inflation. We present a general formula for both the stochastic and the non-stochastic parts of the halo bias, in terms of the N-point cumulants of the curvature perturbation at the end of inflation. At lowest order, the stochasticity arises if the collapsed limit of the four-point function is boosted relative to the square of the three-point function in the squeezed limit. We derive all our results in two ways, using the barrier crossing formalism and the peak-background split method. In a companion paper [1], we prove that these two approaches are mathematically equivalent.

Contents

1 Introduction

A central goal of modern cosmology is to uncover the physics that generated the primordial density perturbations and thereby seeded the large-scale structures (LSS) we see around us. The coherent nature of the cosmic microwave background (CMB) anisotropies suggests that the fluctuations were created at very early times, possibly during a period of inflation [2].

One of the few observational probes that allows us access to the physics of that epoch is primordial non-Gaussianity [3]. At present, the best constraints on non-Gaussianity are coming from the CMB (e.g. [4]), but LSS is emerging as a promising complementary observable (e.g. [5, 6]). Historically, the usefulness of LSS as a tool for early universe cosmology has been viewed with some suspicion, since non-linear evolution can itself produce significant non-Gaussianity even if the initial conditions were perfectly Gaussian. Disentangling any primordial non-Gaussianity from these late time effects always seemed like a messy business. This attitude has changed somewhat when it was discovered that non-Gaussian initial conditions lead to a *scale-dependent* clustering of galaxies on large scales [7, 8]. In particular, it was shown that non-linear mode coupling induces a modulation of the local short-scale power $\sigma_8(\boldsymbol{x})$ by the long-wavelength gravitational potential $\Phi(\boldsymbol{x})$. This results in a biasing of halos (or galaxies) that is proportional to Φ rather than the dark matter density δ (or $\nabla^2\Phi$). Crucially, the appearance of Φ rather than δ in the halo bias implies a specific form of scale-dependence that cannot be created dynamically (i.e. by late time processes). This is the main reason that halo bias is such a robust probe of the initial conditions.

Figure 1: *The squeezed limit of the three-point function, $k_1 \to 0$, gives the dominant contribution to the scale-dependent halo bias. A stochastic form of scale-dependent halo bias arises if the four-point function is large in the collapsed limit, $k_{12} \equiv |\boldsymbol{k}_1 + \boldsymbol{k}_2| \to 0$.*

In this paper, we study *stochastic* halo bias on large scales. The term 'stochastic' here refers to the fact that the halo over-density is not 100% correlated to the matter over-density on large scales, i.e. the halo-halo power spectrum $P_{\rm hh}(k)$ is boosted relative to the matter-halo power spectrum $P_{\rm mh}(k)$. Formally, this means that

$$P_{\rm hh}(k) > b^2(k) P_{\rm mm}(k) + \frac{1}{n_{\rm h}} \,, \tag{1.1}$$

where $b(k) \equiv P_{\rm mh}(k)/P_{\rm mm}(k)$ is the halo bias, and $n_{\rm h}$ is the halo number density. Large-scale stochastic bias arises in non-Gaussian models when the small-scale power $\sigma_8(\boldsymbol{x})$ varies from point to point, but in a way that isn't completely correlated with the local value of $\Phi(\boldsymbol{x})$ and its derivatives. This is most easily demonstrated in models with multiple fields, where the small-scale power may depend on fields that do not contribute to the (linearized) gravitational potential. Our goal in this paper is to provide an understanding of the origin of stochastic bias in a model-independent way. In the absence of significant isocurvature perturbations, all the relevant information must

be encoded in the correlation functions of gravitational potential Φ. It will be useful to define

$$\hat{f}_{\rm NL} \equiv \frac{1}{4} \lim_{k_1 \to 0} \frac{\xi_\Phi^{(3)}(\boldsymbol{k}_1, \boldsymbol{k}_2, \boldsymbol{k}_3)}{P_1 P_2} \ , \tag{1.2}$$

$$\hat{\tau}_{\rm NL} \equiv \frac{9}{100} \lim_{k_{12} \to 0} \frac{\xi_\Phi^{(4)}(\boldsymbol{k}_1, \boldsymbol{k}_2, \boldsymbol{k}_3, \boldsymbol{k}_4)}{P_1 P_3 P_{12}} \ , \tag{1.3}$$

where $\langle \Phi_{\boldsymbol{k}_1} \cdots \Phi_{\boldsymbol{k}_N} \rangle_{\rm c} \equiv (2\pi)^3 \xi_\Phi^{(N)}(\boldsymbol{k}_1, \cdots, \boldsymbol{k}_n)\, \delta_{\rm D}(\boldsymbol{k}_1 + \cdots + \boldsymbol{k}_n)$ and $P_i \equiv \xi_\Phi^{(2)}(k_i)$. This parametrizes the amplitude of the three-point function in the *squeezed limit*, $k_1 \ll \min\{k_2, k_3\}$, and the amplitude of the four-point function in the *collapsed limit*, $k_{12} \equiv |\boldsymbol{k}_1 + \boldsymbol{k}_2| \ll \min\{k_i\}$. As we will show, stochastic bias arises if the 'collapsed four-point function' is *not* equal to the square of the 'squeezed three-point function', i.e. if $\hat{\tau}_{\rm NL} \neq (\frac{6}{5}\hat{f}_{\rm NL})^2$. There exists a well-known theoretical constraint on the relative size of $\hat{\tau}_{\rm NL}$ and $(\frac{6}{5}\hat{f}_{\rm NL})^2$. If only a single field (which may or may not be the inflaton) generates the primordial curvature perturbation and its non-Gaussianity, then $\hat{\tau}_{\rm NL} = (\frac{6}{5}\hat{f}_{\rm NL})^2$ [9] and the biasing is non-stochastic. On the other hand, if multiple coupled fields generate the non-Gaussianity, then $\hat{\tau}_{\rm NL}$ can be larger[1] than $(\frac{6}{5}\hat{f}_{\rm NL})^2$ [16, 17] and the biasing will be stochastic. We will discuss classes of inflationary theories that predict precisely this kind of observational signature [18–20]. This provides the opportunity of using scale-dependent stochastic bias[2] as a probe of any early universe physics associated with a boosted collapsed four-point function—just like the non-stochastic scale-dependent bias is a powerful probe of the squeezed three-point function.

More generally, we find that the large-scale non-stochastic bias can be written as a sum over N-point functions $\xi_\Phi^{(N)}(\boldsymbol{k}_1, \cdots, \boldsymbol{k}_N)$ evaluated in the squeezed limit $k_1 \ll \min\{k_2, \cdots, k_N\}$.[3] The stochastic bias, on the other hand, involves a double sum over $(M+N)$-point functions $\xi_\Phi^{(M+N)}(\boldsymbol{k}_1, \cdots, \boldsymbol{k}_{M+N})$ evaluated in the collapsed limit $|\boldsymbol{k}_1 + \cdots + \boldsymbol{k}_M| \ll \min\{k_i\}$. Stochastic bias arises if any collapsed $(M+N)$-point function is boosted relative to the product of the corresponding squeezed $(M+1)$-point and $(N+1)$-point functions. In all physically interesting cases that we are aware of, this effect is due to the collapsed four-point function being boosted relative to the square of the three-point function (i.e. the case $M = N = 2$). Therefore, we will generally interpret stochastic bias as a probe of the collapsed four-point function. The main result of this paper is a general pair of formulas, eqs. (3.26) and (3.36), for the non-stochastic and stochastic parts of the bias, for completely general non-Gaussian initial conditions parametrized by the N-point cumulants $\xi_\Phi^{(N)}(\boldsymbol{k}_1, \cdots, \boldsymbol{k}_N)$.

The outline of the paper is as follows: We will begin, in Section 2, with a qualitative explanation of scale-dependent stochastic bias. In Section 3, we will show how our intuitive understanding

[1] No matter how the fluctuations were created, the parameters have to satisfy the Suyama-Yamaguchi inequality $\hat{\tau}_{\rm NL} \geq (\frac{6}{5}\hat{f}_{\rm NL})^2$ [10] (see also [11–15]). This is easy to understand: we can think of $\hat{f}_{\rm NL}$ as a measure of the large-scale correlation between the potential Φ and the locally measured small-scale power, $\hat{f}_{\rm NL} \sim \langle \Phi_\ell \Phi_s^2 \rangle / \langle \Phi_\ell^2 \rangle \langle \Phi_s^2 \rangle$. On the other hand, $\hat{\tau}_{\rm NL}$ is a measure of the large-scale variance in the small-scale power, $\hat{\tau}_{\rm NL} \sim \langle \Phi_s^2 \Phi_s^2 \rangle_{\rm c} / \langle \Phi_\ell^2 \rangle \langle \Phi_s^2 \rangle^2$. The inequality $\hat{\tau}_{\rm NL} \geq (\frac{6}{5}\hat{f}_{\rm NL})^2$ then arises simply as the condition that the correlation coefficient between the small-scale power and Φ must be between -1 and 1.

[2] We should note that in this paper we are interested in large-scale stochastic bias. On small scales, non-linear evolution and astrophysical processes can create local stochasticity, which is not relevant in our study.

[3] More precisely, k_1 is fixed to the large scale k where we are computing the bias, and $k_2, \cdots, k_N$ are integrated over a broad range of scales near the halo collapse scale $k_{\rm h} \sim \rho_{\rm m}^{1/3} M^{-1/3}$.

is borne out in the barrier crossing model of structure formation. In Section 4, we will illustrate these results with explicit examples. In each case, we also derive our predictions in the peak-background split formalism. In a companion paper [1], we prove the mathematical equivalence of barrier crossing and peak-background split. We present our conclusions in Section 5. Finally, Appendix A discusses the convergence of the Edgeworth expansion for local non-Gaussianity.

2 Stochastic Bias

Galaxies reside in dark matter halos. For Gaussian initial conditions and at long wavelengths, the fluctuations in the density of halos $\delta_{\rm h}$ can be expressed as an expansion in the linear matter density field δ. At linear order, the two are simply related by a numerical factor—the bias b_g—i.e. $\delta_{\rm h} = b_g\delta$. This simple bias relation gets modified for non-Gaussian initial conditions, due to a coupling between short and long-wavelength modes. The short modes determine the collapse of dark matter halos, while long modes modulate the density on large scales, effectively raising or lowering the threshold for the formation of collapsed objects. A non-zero three-point function affects the variance of the short modes, leading to a dependence of the number density of halos on the amplitude of the long modes. For local non-Gaussianity[4] this leads to a dependence of the halo density on the long-wavelength gravitational potential Φ rather than the matter density $\delta \propto \nabla^2\Phi$. This leads to a characteristic *scale-dependence* in the bias relation, $\Delta b \propto k^{-2}$ [7]. It is this scale-dependence that allows us to trust the large-scale bias as a probe of initial conditions. Crucially, the dependence of the halo density on Φ is not something that could be mimicked by local dynamics. Dynamical processes don't care about the local value of the potential, but are only sensitive to tidal forces which are proportional to $\nabla^2\Phi$ and $\dot{\Phi}$ (essentially this is a consequence of the equivalence principle). Any dependence of the small-scale power on Φ itself can therefore only come from the initial conditions. This is what makes scale-dependent bias such a promising probe of early universe physics, despite all the astrophysical uncertainties associated with galaxy formation.

Stochastic bias arises whenever the density of halos is not 100% correlated with the potential Φ or its derivatives. In order to develop some intuition, we now give a schematic derivation of the effect. In the next section, we will upgrade this to a more formal analysis in the barrier crossing approach. If we assume that the primordial perturbations are adiabatic, then the formation of halos can only depend on local physics of the fluctuations. Nevertheless, long-wavelength variations of the number of halos may depend, not only on the local value of the linear density field, but on all of its local correlation functions. Assuming only locality, we may therefore write the local halo number density as

$$n_{\rm h}(\boldsymbol{x}) = \bar{n}_{\rm h}(\delta(\boldsymbol{x}); [\delta^n](\boldsymbol{x})) \ , \tag{2.1}$$

where $[...]$ denotes an average over a small region of characteristic size ℓ that is centered around $\boldsymbol{x}$. Long-wavelength fluctuations in the number of halos can then be understood as a Taylor expansion,

$$\delta_{\rm h}(\boldsymbol{x}) \equiv \frac{\delta n_{\rm h}}{\bar{n}_{\rm h}} = b_g\delta(\boldsymbol{x}) + \beta[\delta^2](\boldsymbol{x}) + \cdots \ , \tag{2.2}$$

[4] In real space, local non-Gaussianity is parametrized as $\Phi(\boldsymbol{x}) = \phi(\boldsymbol{x}) + f_{\rm NL}(\phi^2(\boldsymbol{x}) - \langle\phi^2\rangle)$, where ϕ is Gaussian.

where b_g is the Gaussian bias and

$$\beta \equiv \frac{\partial \ln n_{\rm h}}{\partial [\delta^2]} \ . \tag{2.3}$$

It is easy to see (e.g. by splitting all fields into long and short modes), that for local non-Gaussianity the short-scale power is modulated by the gravitational potential, $[\delta^2] \approx [\delta^2]_g\,(1 + 4 f_{\rm NL}\Phi(\boldsymbol{x}))$. This is the origin of scale-dependent bias in local non-Gaussianity.

Using the expansion (2.2), we can also evaluate correlation functions between two spatially separated points $\boldsymbol{x}$ and $\boldsymbol{x}'$. We use a prime to indicate that fields are evaluated at $\boldsymbol{x}'$, while fields without a prime are evaluated at $\boldsymbol{x}$. The matter-halo correlation, in a large region of size $L \gg \ell$, then is

$$\frac{\langle \delta_{\rm h} \delta' \rangle}{\langle \delta \delta' \rangle} = b_g + \beta \frac{\langle [\delta^2]\, \delta' \rangle}{\langle \delta \delta' \rangle} + \cdots \ , \tag{2.4}$$

while the halo-halo correlation is

$$\frac{\langle \delta_{\rm h} \delta_{\rm h}{}' \rangle}{\langle \delta \delta' \rangle} = b_g^2 + 2 b_g \beta \frac{\langle [\delta^2]\, \delta' \rangle}{\langle \delta \delta' \rangle} + \beta^2 \frac{\langle [\delta^2] [\delta^2]' \rangle}{\langle \delta \delta' \rangle} + \cdots \ . \tag{2.5}$$

This leads to the possibility that the bias inferred from $\langle \delta_{\rm h} \delta \rangle$ is not equal to the bias inferred from $\langle \delta_{\rm h} \delta_{\rm h}{}' \rangle$. We characterize this so-called stochasticity of the halo bias by the following parameter[5]

$$r \equiv \frac{\langle \delta_{\rm h} \delta_{\rm h}{}' \rangle}{\langle \delta \delta' \rangle} - \left(\frac{\langle \delta_{\rm h} \delta' \rangle}{\langle \delta \delta' \rangle} \right)^2 \ . \tag{2.6}$$

Using eqs. (2.4) and (2.5), we find

$$r = \beta^2 \left[\frac{\langle [\delta^2] [\delta^2]' \rangle}{\langle \delta \delta' \rangle} - \left(\frac{\langle [\delta^2]\, \delta' \rangle}{\langle \delta \delta' \rangle} \right)^2 \right] + \cdots \ . \tag{2.7}$$

This simple argument gives reliable intuition for the origin of stochasticity. Specifically, we see that if a local variation in the amplitude of $[\delta^2](\boldsymbol{x})$ is uncorrelated with $\delta(\boldsymbol{x}')$, then there is no extra contribution to the bias in eq. (2.4). Nevertheless, the halo-halo correlation function in eq. (2.5) can still be modified by long-wavelength variations in $[\delta^2](\boldsymbol{x})$. Moreover, the result (2.7) makes it clear that stochasticity arises from a non-trivial four-point function of the primordial potential. In fact, the real space correlation function $\langle [\delta^2](\boldsymbol{x}) [\delta^2](\boldsymbol{x}') \rangle$ relates to the collapsed limit of the four-point function in Fourier space, i.e. $\lim_{|\boldsymbol{k}_1 + \boldsymbol{k}_2| \to 0} \langle \Phi_{\boldsymbol{k}_1} \Phi_{\boldsymbol{k}_2} \Phi_{\boldsymbol{k}_3} \Phi_{\boldsymbol{k}_4} \rangle$.

3 Predictions from Barrier Crossing

In this section, we give a formal derivation of stochastic bias using the classic barrier crossing method of Press and Schechter [21]. Our goal is to obtain an expression for the stochasticity coefficient (2.6) in terms of the cumulants of the smoothed density field. These in turn can be related to N-point functions of the primordial potential and hence contain information about the initial conditions.

[5] In practice, we also have to subtract shot noise contributions from $\langle \delta_{\rm h} \delta_{\rm h}{}' \rangle$ and $\langle \delta_{\rm h} \delta' \rangle$—see §3.3.

3.1 Definitions and Notation

We begin with some basic definitions and a description of our notation. Let $\hat{\delta}(\boldsymbol{x}, z)$ denote the linear density field (to be distinguished by the hat from the non-linear density field δ). The linearized Poisson equation relates $\hat{\delta}$ to the primordial potential Φ,

$$\hat{\delta}_{\boldsymbol{k}}(z) = \alpha(k, z)\Phi_{\boldsymbol{k}} \ , \tag{3.1}$$

where

$$\alpha(k, z) \equiv \frac{2}{3}\frac{k^2}{\Omega_m H_0^2}\, T(k)D(z) \ . \tag{3.2}$$

Here, $T(k)$ is the matter transfer function normalized such that $T(k) \to 1$ as $k \to 0$ and $D(z)$ is the linear growth factor (as function of redshift z), normalized so that $D(z) = (1+z)^{-1}$ in matter domination. For notational simplicity, we will from now on suppress the redshift argument from all quantities. We use $\delta_{\scriptscriptstyle M}(\boldsymbol{x})$ for the linear field smoothed with a top-hat window function with radius[6] $R_{\scriptscriptstyle M} \equiv (3M/4\pi\bar{\rho}_{\rm m})^{1/3}$, so that

$$\delta_{\scriptscriptstyle M}(\boldsymbol{x}) = \int_{\boldsymbol{k}} e^{-i\boldsymbol{k}\cdot\boldsymbol{x}}\, W_{\scriptscriptstyle M}(k)\hat{\delta}_{\boldsymbol{k}} = \int_{\boldsymbol{k}} e^{-i\boldsymbol{k}\cdot\boldsymbol{x}}\, \alpha_{\scriptscriptstyle M}(k)\Phi_{\boldsymbol{k}} \ , \tag{3.3}$$

where $\int_{\boldsymbol{k}}(\cdot) \equiv \int \frac{{\rm d}^3\boldsymbol{k}}{(2\pi)^3}(\cdot)$,

$$W_{\scriptscriptstyle M}(k) \equiv 3\,\frac{\sin(kR_{\scriptscriptstyle M}) - kR_{\scriptscriptstyle M}\cos(kR_{\scriptscriptstyle M})}{(kR_{\scriptscriptstyle M})^3} \ , \tag{3.4}$$

and $\alpha_{\scriptscriptstyle M}(k) \equiv W_{\scriptscriptstyle M}(k)\alpha(k)$. Let $\sigma_{\scriptscriptstyle M} = \langle\delta_{\scriptscriptstyle M}^2\rangle^{1/2}$ be the rms amplitude of the smoothed density field, and $\kappa_n(M)$ be its n-th non-Gaussian cumulant,

$$\kappa_n(M) = \frac{\langle\delta_{\scriptscriptstyle M}^n\rangle_{\rm c}}{\sigma_{\scriptscriptstyle M}^n} \ , \tag{3.5}$$

where the subscript 'c' indicates the use of a connected correlation function. Since $\delta_{\scriptscriptstyle M}$ and $\sigma_{\scriptscriptstyle M}$ are defined via linear theory, $\kappa_n(M)$ is independent of redshift. Similar definitions apply to the unsmoothed field $\hat{\delta}$, in which case we denote the variance and cumulants by $\hat{\sigma}$ and $\kappa_{\hat{n}}$.

Ultimately, we will be interested in two-point clustering statistics. Let $\boldsymbol{x}$ and $\boldsymbol{x}'$ be two points separated by a distance $r \equiv |\boldsymbol{x} - \boldsymbol{x}'|$. Moreover, let a prime indicate that the field is evaluated at $\boldsymbol{x}'$, e.g. $\delta'_{\scriptscriptstyle M} \equiv \delta_{\scriptscriptstyle M}(\boldsymbol{x}')$. Fields without a prime are evaluated at $\boldsymbol{x}$. The joint cumulants are then defined by

$$\kappa_{\hat{m},n}(r, M) \ \equiv \ \frac{\langle\hat{\delta}^m(\delta'_{\scriptscriptstyle M})^n\rangle_{\rm c}}{\hat{\sigma}^m\sigma_{\scriptscriptstyle M}^n} \ , \tag{3.6}$$

$$\kappa_{m,n}(r, M, \bar{M}) \ \equiv \ \frac{\langle(\delta_{\scriptscriptstyle M})^m(\delta'_{\bar{M}})^n\rangle_{\rm c}}{\sigma_{\scriptscriptstyle M}^m\sigma_{\bar{M}}^n} \ . \tag{3.7}$$

These cumulants can be related to N-point functions of the gravitational potential,

$$\langle\Phi_{\boldsymbol{k}_1}\Phi_{\boldsymbol{k}_2}\cdots\Phi_{\boldsymbol{k}_N}\rangle_{\rm c} = (2\pi)^3\delta_{\rm D}(\boldsymbol{k}_{12\ldots N})\,\xi_\Phi^{(N)}(\boldsymbol{k}_1, \boldsymbol{k}_2, \ldots, \boldsymbol{k}_N) \ , \tag{3.8}$$

where $\boldsymbol{k}_{12\ldots N} \equiv \boldsymbol{k}_1 + \boldsymbol{k}_2 + \cdots + \boldsymbol{k}_N$.

[6] The smoothing scale $R_{\scriptscriptstyle M}$ corresponds to the comoving size of halos of mass M in Lagrangian space.

3.2 Edgeworth Expansions

The probability density functions (PDFs) of weakly non-Gaussian random variables have well-defined Edgeworth expansions (for a review see e.g. [22]). Consider first the variables $\delta_{_M}$ and $\delta'_{_M}$. It will be convenient to define the rescaled fields

$$\nu \equiv \frac{\delta_{_M}}{\sigma_{_M}} \qquad \text{and} \qquad \nu' \equiv \frac{\delta'_{_M}}{\sigma_{_M}} \ , \tag{3.9}$$

with $\langle\nu\rangle = \langle\nu'\rangle = 0$ and $\langle\nu^2\rangle = \langle(\nu')^2\rangle = 1$. The cumulants in eqs. (3.5) and (3.7) then become $\kappa_n = \langle\nu^n\rangle_{\rm c}$ and $\kappa_{m,n} = \langle\nu^m(\nu')^n\rangle_{\rm c}$. The Edgeworth expansion for the marginal PDF is

$$p(\nu) = \exp\left(\sum_{n\geq 3}\frac{(-1)^n}{n!}\kappa_n\frac{\partial^n}{\partial\nu^n}\right)p_g(\nu) \ , \qquad \text{where} \quad p_g(\nu) \equiv \frac{1}{\sqrt{2\pi}}e^{-\frac{1}{2}\nu^2} \ . \tag{3.10}$$

The first few terms can be written as

$$p(\nu) \ = \ \left(1 + \frac{\kappa_3}{3!}H_3(\nu) + \frac{\kappa_4}{4!}H_4(\nu) + \cdots\right)p_g(\nu) \ , \tag{3.11}$$

where the functions $H_n(\nu)$ are Hermite polynomials

$$H_n(\nu) \equiv (-1)^n e^{\frac{1}{2}\nu^2}\frac{d^n}{d\nu^n}e^{-\frac{1}{2}\nu^2} \ . \tag{3.12}$$

Similarly, the Edgeworth expansion for the joint PDF is

$$p(\nu,\nu') = \exp\left(\kappa_{1,1}\frac{\partial^2}{\partial\nu\partial\nu'} + \sum_{m+n\geq 3}\frac{(-1)^{m+n}}{m!n!}\kappa_{m,n}\frac{\partial^{m+n}}{\partial\nu^m\partial(\nu')^n}\right)p_g(\nu)p_g(\nu') \ . \tag{3.13}$$

In Appendix A, we discuss the convergence properties of this expansion. In the next section, we will use it to compute halo-halo correlations.

The matter-halo case is completely analogous: to construct the joint PDF of the variables $\hat{\delta}$ and $\delta'_{_M}$, we define rescaled variables $\hat{\nu} = \hat{\delta}/\hat{\sigma}$ and $\nu' = \delta'_{_M}/\sigma_{_M}$. The joint PDF $p(\hat{\nu},\nu')$ is then given by the Edgeworth series (3.13) with the cumulant $\kappa_{m,n}$ replaced by $\kappa_{\hat{m},n}$.

3.3 Barrier Crossing

In the simplest version of the barrier crossing formalism [21], halos of mass $\geq M$ are identified with regions where the *linearly* evolved smoothed density field exceeds a constant threshold value δ_c for collapse. The halo number density $n_{\rm h}(\boldsymbol{x})$ is then given by

$$n_{\rm h}(\boldsymbol{x}) = 2\,\frac{\bar{\rho}_{\rm m}}{M}\,\Theta(\delta_{_M}(\boldsymbol{x}) - \delta_c) \ , \tag{3.14}$$

with Θ the Heaviside step function. It has been shown numerically that $\delta_c \approx 1.42$ produces good results [23], but for our analytical calculations we don't need to specify a particular value for δ_c. The fraction of space occupied by regions above the collapse threshold is

$$f(M) = \int_{\nu_c}^{\infty}[{\rm d}\nu]\ p(\nu) \ , \tag{3.15}$$

where $\nu_c(M) \equiv \delta_c/\sigma_M$. Using the Edgeworth expansion (3.11), we find[7]

$$f(M) = \frac{1}{2}\,\mathrm{erfc}\left(\frac{\nu_c}{\sqrt{2}}\right) + p_g(\nu_c)\left[\frac{\kappa_3(M)}{3!}H_2(\nu_c) + \frac{\kappa_4(M)}{4!}H_3(\nu_c) + \cdots\right] . \tag{3.16}$$

When interpreting calculations in the barrier crossing model, it must be kept in mind that eq. (3.14) for $n_{\rm h}(\boldsymbol{x})$ is the number density of halos in *Lagrangian* space. Our convention throughout this paper is that the power spectra $P_{\rm mh}(k)$ and $P_{\rm hh}(k)$ are always computed in Lagrangian space. In particular, b_g denotes the Lagrangian bias. The relevant quantity to compare to observations or simulations is the *Eulerian* bias which, to lowest order, is given by $b_g^{\rm E} = 1 + b_g$.

The barrier crossing model also neglects shot noise contributions which arise from the finite halo number density $n_{\rm h}$. Throughout this paper, $P_{\rm hh}$ always denotes the halo-halo power spectrum after subtracting the shot noise contribution $1/n_{\rm h}$. (There are also shot noise, or one-halo, contributions to the matter-halo power spectrum $P_{\rm mh}$, which are usually negligible, but are a leading source of stochastic bias in the Gaussian case [24, 25].)

3.3.1 Matter-Halo Correlations

The correlation between the halo field at $\boldsymbol{x}'$ and the dark matter field at $\boldsymbol{x}$ is given by

$$\hat{\xi}(r, M) \;=\; \frac{M}{2\bar{\rho}_{\rm m}}\int_{-\infty}^{\infty}[\mathrm{d}\hat{\delta}]\int_{-\infty}^{\infty}[\mathrm{d}\delta'_M]\,\hat{\delta}(\boldsymbol{x})\,n_{\rm h}(\boldsymbol{x}')\,p(\hat{\delta}, \delta'_M)\ . \tag{3.17}$$

In the rescaled variables $\hat{\nu} \equiv \hat{\delta}(\boldsymbol{x})/\hat{\sigma}$ and $\nu' \equiv \delta_M(\boldsymbol{x}')/\sigma_M$, this becomes

$$\hat{\xi}(r, M) \;=\; \hat{\sigma}\int_{-\infty}^{\infty}[\mathrm{d}\hat{\nu}]\int_{\nu_c}^{\infty}[\mathrm{d}\nu']\,\hat{\nu}\,p(\hat{\nu}, \nu')\ . \tag{3.18}$$

It will be convenient to work in momentum space via $\hat{\xi}(k, M) = \int \mathrm{d}^3\boldsymbol{r}\, e^{i\boldsymbol{k}\cdot\boldsymbol{r}}\hat{\xi}(r, M)$. To describe the correlations of halos in the mass bin $[M, M + \mathrm{d}M]$, we take derivatives with respect to M. The matter-halo power spectrum is then given by

$$P_{\rm mh}(k, M) = \frac{d\hat{\xi}(k, M)}{dM}\left(\frac{df(M)}{dM}\right)^{-1} . \tag{3.19}$$

To compute the correlation function (3.18), we substitute the Edgeworth expansion (3.13) for $p(\hat{\nu}, \nu')$. Only terms with exactly one $\hat{\nu}$-derivative survive the integration, and we therefore find

$$\hat{\xi}(k, M) = \hat{\sigma}\,p_g(\nu_c)\left[\kappa_{\hat{1},1} + \frac{H_1(\nu_c)}{2!}\kappa_{\hat{1},2} + \frac{H_2(\nu_c)}{3!}\kappa_{\hat{1},3} + \frac{H_3(\nu_c)}{3!}\kappa_{\hat{1},1}\star\kappa_3 + \cdots\right] , \tag{3.20}$$

where $\star$ denotes a convolution. We see that the matter-halo correlations, or equivalently the non-stochastic part of the halo bias, only depend on the following cumulants

$$\kappa_{\hat{1},n}(k, M) = \hat{\sigma}^{-1}\sigma_M^{-n}\left(\prod_{i=1}^{n}\int_{\boldsymbol{q}_i}\alpha_M(q_i)\right)\alpha(k)\langle\Phi_{\boldsymbol{k}}\Phi_{\boldsymbol{q}_1}\cdots\Phi_{\boldsymbol{q}_n}\rangle_{\rm c}\ . \tag{3.21}$$

[7] In our notation the halo mass function is $dn_{\rm h}/dM = -\bar{\rho}_{\rm m}/M(df/dM)$.

Moreover, we note that the large-scale limit, $\lim_{k\to 0}\kappa_{\hat{1},n}(k,M)$, is determined by the squeezed limit of the primordial $(n+1)$-point function [26],

$$\lim_{k\to 0}\xi_\Phi^{(n+1)}(\boldsymbol{k},\boldsymbol{q}_1,\cdots,\boldsymbol{q}_n)\ . \tag{3.22}$$

The explicit form of the cumulants $\kappa_{\hat{1},n\geq 2}$ depends on the type of non-Gaussianity. We compute some examples in Section 4.

Keeping only linear terms[8] in eq. (3.20), we get

$$\hat{\xi}(k,M)=p_g(\nu_c)(\kappa_{\hat{1},1}\hat{\sigma}\sigma_M)\left[\frac{1}{\sigma_M}+\sum_{n=2}^{\infty}\frac{H_{n-1}(\nu_c)}{n!}f_{\hat{1},n}+\cdots\right]\ , \tag{3.23}$$

where we defined

$$f_{\hat{1},n}(k,M)\equiv\frac{\kappa_{\hat{1},n}(k,M)}{\kappa_{\hat{1},1}(k,M)\,\sigma_M}\ . \tag{3.24}$$

It was convenient to factor out the Gaussian term $\kappa_{\hat{1},1}\hat{\sigma}\sigma_M$, since at long wavelengths it becomes the matter power spectrum

$$\kappa_{\hat{1},1}\,\hat{\sigma}\sigma_M=\int_{\boldsymbol{q}}\alpha(k)\alpha_M(q)\langle\Phi_{\boldsymbol{k}}\Phi_{\boldsymbol{q}}\rangle=W_M(k)P_{\rm mm}(k)\ \xrightarrow{k\to 0}\ P_{\rm mm}(k)\ . \tag{3.25}$$

Evaluating eq. (3.19), we find

$$P_{\rm mh}(k)\ \xrightarrow{k\to 0}\ P_{\rm mm}(k)\left[b_g+\sum_{n=2}^{\infty}\left(\beta_n+\tilde{\beta}_n\frac{d}{d\ln\sigma_M}\right)f_{\hat{1},n}+\cdots\right]\ , \tag{3.26}$$

where

$$b_g\equiv\frac{1}{\sigma_M}\frac{\nu_c^2-1}{\nu_c}\quad,\quad\beta_n\equiv\frac{H_n(\nu_c)}{n!}\quad\text{and}\quad\tilde{\beta}_n\equiv\frac{H_{n-1}(\nu_c)}{n!\,\nu_c}\ . \tag{3.27}$$

The ellipses in eq. (3.26) stand for terms that are non-linear in the cumulants. For local non-Gaussianity, the derivative terms $df_{\hat{1},n}/d\ln\sigma_M$ will be negligible, but in principle, we can keep them (and sometimes we have to).

Our expression (3.26) agrees with the general formula for the non-stochastic bias given in [26]; however, ref. [26] implicitly found that non-Gaussianity cannot generate large-scale stochastic bias. In the next section, we will find the opposite conclusion. The disagreement is easy to understand: Ref. [26] claims after their eq. (40) that contributions to $P_{\rm hh}$ from cumulants $\kappa_{m,n}$ with $m,n\geq 2$ must approach a constant as $k\to 0$. This is not true for general non-Gaussian initial conditions and exceptions to that statement are precisely what causes the effects discuss in this paper.

[8] In Appendix A, we explain that the lowest order cumulants usually dominate and that products of cumulants are suppressed.

3.3.2 Halo-Halo Correlations

Next, we consider the correlation between the halo fields at $\boldsymbol{x}$ and $\boldsymbol{x}'$,

$$\xi(r, M, \bar{M}) \;=\; \frac{M\bar{M}}{4\bar{\rho}_{\rm m}^2}\int_{-\infty}^{\infty}[{\rm d}\delta_M]\int_{-\infty}^{\infty}[{\rm d}\delta'_{\bar{M}}]\, n_{\rm h}(\boldsymbol{x})n_{\rm h}(\boldsymbol{x}')\, p(\delta_M, \delta'_{\bar{M}})\ . \tag{3.28}$$

In the rescaled variables $\nu \equiv \delta_M(\boldsymbol{x})/\sigma_M$ and $\nu' \equiv \delta_{\bar{M}}(\boldsymbol{x}')/\sigma_{\bar{M}}$, this becomes

$$\xi(r, M, \bar{M}) \;=\; \int_{\nu_c}^{\infty}[{\rm d}\nu]\int_{\bar{\nu}_c}^{\infty}[{\rm d}\nu']\; p(\nu, \nu')\ . \tag{3.29}$$

Notice that, in principle, we have allowed for two distinct mass thresholds, M and $\bar{M}$. The power spectrum of halos in the mass bins $[M, M + {\rm d}M]$ and $[\bar{M}, \bar{M} + {\rm d}\bar{M}]$ then is

$$P_{\rm h\bar{h}}(k) = \frac{d^2\xi(k, M, \bar{M})}{dMd\bar{M}}\left(\frac{df(M)}{dM}\frac{df(\bar{M})}{d\bar{M}}\right)^{-1}\ . \tag{3.30}$$

For simplicity, we will restrict the following presentation to correlations of equal mass halos, $M = \bar{M}$. The power spectrum for a narrow mass bin around M is then given by

$$P_{\rm hh}(k) = \left.\frac{d^2\xi(k, M, \bar{M})}{dMd\bar{M}}\right|_{\bar{M}=M}\left(\frac{df(M)}{dM}\right)^{-2}\ . \tag{3.31}$$

To compute the correlation function (3.29), we substitute the Edgeworth expansion (3.13) for $p(\nu, \nu')$,

$$\begin{aligned}\xi(k, M, \bar{M}) = p_g(\nu_c)p_g(\bar{\nu}_c)\Bigg[\kappa_{1,1} + \frac{1}{2}\big(\kappa_{2,1}H_1(\nu_c) + \kappa_{1,2}H_1(\bar{\nu}_c)\big) + \frac{1}{6}\big(\kappa_{3,1}H_2(\nu_c) + \kappa_{1,3}H_2(\bar{\nu}_c)\big)\\ + \frac{1}{4}\kappa_{2,2}H_1(\nu_c)H_1(\bar{\nu}_c) + \frac{1}{2}\kappa_{1,1}\star\kappa_{1,1} + \cdots\Bigg]\ .\end{aligned} \tag{3.32}$$

The form of higher-order cumulants, such as $\kappa_{1,2}$, $\kappa_{1,3}$ and $\kappa_{2,2}$, again depends on the type of non-Gaussianity. We compute some examples in Section 4.

Keeping only the terms linear in $\kappa_{m,n}$ (this approximation will be justified in Appendix A) in eq. (3.32), we find

$$\begin{aligned}\xi(k, M, \bar{M}) \;=\; p_g(\nu_c)p_g(\bar{\nu}_c)(\kappa_{1,1}\sigma_M\sigma_{\bar{M}})\Bigg[\frac{1}{\sigma_M\sigma_{\bar{M}}} + \sum_{n=2}^{\infty}\left(\frac{1}{\sigma_M}\frac{H_{n-1}(\bar{\nu}_c)}{n!}\, f_{1,n} + \frac{1}{\sigma_{\bar{M}}}\frac{H_{n-1}(\nu_c)}{n!}\, f_{n,1}\right)\\ + \sum_{m=2}^{\infty}\sum_{n=2}^{\infty}\frac{H_{m-1}(\nu_c)}{m!}\frac{H_{n-1}(\bar{\nu}_c)}{n!}f_{m,n} \;+\; \cdots\Bigg]\ ,\end{aligned} \tag{3.33}$$

where

$$f_{1,n}(k, M, \bar{M}) \equiv \frac{\kappa_{1,n}(k, M, \bar{M})}{\kappa_{1,1}(k, M, \bar{M})\sigma_{\bar{M}}} \qquad \text{for } n \geq 1\ , \tag{3.34}$$

$$f_{m,n}(k, M, \bar{M}) \equiv \frac{\kappa_{m,n}(k, M, \bar{M})}{\kappa_{1,1}(k, M, \bar{M})\sigma_M\sigma_{\bar{M}}} \qquad \text{for } m, n \geq 2\ . \tag{3.35}$$

We again factored out the Gaussian contribution, $\kappa_{1,1}\,\sigma_M\sigma_{\bar{M}} \xrightarrow{k\to 0} P_{\rm mm}(k)$. Note that $f_{1,n} = f_{\hat{1},n}$ in the large scale limit $k \ll R_M^{-1}$, where $f_{\hat{1},n}$ was defined in eq. (3.24). Substituting (3.33) into (3.31), we get

$$P_{\rm hh}(k) \xrightarrow{k\to 0} P_{\rm mm}(k)\left[b_g^2 + 2b_g\sum_{n=2}^{\infty}\left(\beta_n + \tilde{\beta}_n\frac{\partial}{\partial \ln\sigma_M}\right) f_{1,n} + \sum_{m=2}^{\infty}\sum_{n=2}^{\infty}\left(\beta_m + \tilde{\beta}_n\frac{\partial}{\partial \ln\sigma_M}\right)\left(\beta_m + \tilde{\beta}_n\frac{\partial}{\partial \ln\sigma_{\bar{M}}}\right) f_{m,n} + \cdots\right] . \tag{3.36}$$

Note that, while in the end we always take $M = \bar{M}$ in this paper, M and $\bar{M}$ are independent variables when calculating partial derivatives of $f_{m,n}(M, \bar{M})$.

3.4 Stochastic Halo Bias

We now combine the above results to evaluate the stochasticity coefficient

$$r \equiv \frac{P_{\rm hh}}{P_{\rm mm}} - \left(\frac{P_{\rm mh}}{P_{\rm mm}}\right)^2 , \tag{3.37}$$

where, as usual, it is understood that shot noise is subtracted from $P_{\rm hh}$ and $P_{\rm mh}$. Substituting eqs. (3.26) and (3.36), we find

$$r \xrightarrow{k\to 0} \sum_{m=2}^{\infty}\sum_{n=2}^{\infty}\left(\beta_m + \tilde{\beta}_m\frac{\partial}{\partial \ln\sigma_M}\right)\left(\beta_n + \tilde{\beta}_n\frac{\partial}{\partial \ln\sigma_{\bar{M}}}\right) f_{m,n} - \left[\sum_{n=2}^{\infty}\left(\beta_n + \tilde{\beta}_n\frac{\partial}{\partial \ln\sigma_M}\right) f_{n,1}\right]^2 . \tag{3.38}$$

We note that cumulants $\kappa_{m,n}(k)$ with $m, n \geq 2$ contribute to the halo-halo power spectrum but not the matter-halo power spectrum (3.26), so stochastic halo bias is sourced by these cumulants. These cumulants can be written in terms of the $(m+n)$-point functions of the gravitational potential,

$$\kappa_{m,n}(k, M, \bar{M}) \xrightarrow{k\to 0} \frac{1}{\sigma_M^m\sigma_{\bar{M}}^n}\left(\prod_{i=1}^{m-1}\int_{\boldsymbol{q}_i}\alpha_M(q_i)\right)\left(\prod_{j=1}^{n-1}\int_{\boldsymbol{q}'_j}\alpha_{\bar{M}}(q'_j)\right)\alpha_M(q)\,\alpha_{\bar{M}}(q') \times \xi_\Phi^{(m+n)}\left(\boldsymbol{q}_1, \cdots, \boldsymbol{q}_{m-1}, -\boldsymbol{q}+\boldsymbol{k}, \boldsymbol{q}'_1, \cdots, \boldsymbol{q}'_{n-1}, -\boldsymbol{q}'-\boldsymbol{k}\right) , \tag{3.39}$$

where $\boldsymbol{q} \equiv \sum_{i=1}^{m-1}\boldsymbol{q}_i$ and $\boldsymbol{q}' \equiv \sum_{j=1}^{n-1}\boldsymbol{q}'_j$. We see that, in general, large-scale stochastic bias arises whenever an $(m+n)$-point function $\xi_\Phi^{(m+n)}(\boldsymbol{k}_1, \cdots, \boldsymbol{k}_{m+n})$ is boosted in the collapsed limit $|\sum_{i=1}^{m}\boldsymbol{k}_i| \to 0$, relative to the product of the corresponding squeezed $(m+1)$-point and $(n+1)$-point functions. In the next section, we will compute eq. (3.38) for a few interesting examples. In most cases, we will get stochastic bias from the case $m = n = 2$, i.e. a collapsed four-point function $\lim_{|\boldsymbol{k}_1+\boldsymbol{k}_2|\to 0}\xi_\Phi^{(4)}(\boldsymbol{k}_1, \boldsymbol{k}_2, \boldsymbol{k}_3, \boldsymbol{k}_4)$ which is larger than the square of the squeezed three-point function $\lim_{k_1\to 0}\xi_\Phi^{(3)}(\boldsymbol{k}_1, \boldsymbol{k}_2, \boldsymbol{k}_3)$.

4 Examples

In this section, we discuss several physical mechanisms that lead to stochastic halo bias. For each example, we will derive the result in two different ways:

1) using a peak-background split (PBS) method;

2) using the barrier crossing analysis of the previous section.

We demonstrate explicitly that both approaches lead to the same answers.

4.1 $\tau_{\rm NL}$ Cosmology

A simple phenomenological way to get a boosted collapsed limit for the four-point function is the following generalization of the local ansatz to multiple fields

$$\Phi = A_i\phi_i + B_{ij}\left(\phi_i\phi_j - \langle\phi_i\phi_j\rangle\right) \ , \tag{4.1}$$

with the Einstein summation convention understood. This structure arises, for example, in the curvaton model of [18] (see also [25]),

$$\Phi = \phi + \psi + f_{\rm NL}(1+\Pi)^2\left(\psi^2 - \langle\psi^2\rangle\right) \ , \qquad \text{where} \quad \frac{P_\phi}{P_\psi} \equiv \Pi \ . \tag{4.2}$$

Here, ϕ and ψ are uncorrelated Gaussian random fields with power spectra that are proportional to each other. The three- and four-point functions take the local form

$$\xi^{(3)}_\Phi(\boldsymbol{k}_1,\boldsymbol{k}_2,\boldsymbol{k}_3) = f_{\rm NL}\big[P_1P_2 + 5\,\text{perms.}\big] + \mathcal{O}(f^3_{\rm NL}) \ , \tag{4.3}$$

$$\xi^{(4)}_\Phi(\boldsymbol{k}_1,\boldsymbol{k}_2,\boldsymbol{k}_3,\boldsymbol{k}_4) = 2\left(\tfrac{5}{6}\right)^2\tau_{\rm NL}\big[P_1P_2P_{13} + 23\,\text{perms.}\big] + \mathcal{O}(\tau^2_{\rm NL}) \ , \tag{4.4}$$

where we have defined $P_i \equiv P_\Phi(k_i)$ and $P_{ij} \equiv P_\Phi(|\boldsymbol{k}_i + \boldsymbol{k}_j|)$. However, unlike the single-field local ansatz, now $\tau_{\rm NL}$ need not be equal to $\left(\frac{6}{5}f_{\rm NL}\right)^2$. Instead, the ansatz (4.2) implies $\tau_{\rm NL} \equiv \left(\frac{6}{5}f_{\rm NL}\right)^2(1+\Pi)$, in agreement with the Suyama-Yamaguchi inequality, $\tau_{\rm NL} \geq \left(\frac{6}{5}f_{\rm NL}\right)^2$ [10] (see also [11–15]). The following limits will be useful in computing the cumulants required in the barrier crossing calculation:

$$\lim_{k_1\to 0}\xi^{(3)}_\Phi(\boldsymbol{k}_1,\boldsymbol{k}_2,\boldsymbol{k}_3) = 4f_{\rm NL}P_1P_2 \ , \tag{4.5}$$

$$\lim_{k_1\to 0}\xi^{(4)}_\Phi(\boldsymbol{k}_1,\boldsymbol{k}_2,\boldsymbol{k}_3,\boldsymbol{k}_4) = 8\left(\tfrac{5}{6}\right)^2\tau_{\rm NL}\,P_1\big[P_2P_3 + P_2P_4 + P_3P_4\big] \ , \tag{4.6}$$

$$\lim_{k_{12}\to 0}\xi^{(4)}_\Phi(\boldsymbol{k}_1,\boldsymbol{k}_2,\boldsymbol{k}_3,\boldsymbol{k}_4) = 16\left(\tfrac{5}{6}\right)^2\tau_{\rm NL}\,P_{12}P_1P_3 \ . \tag{4.7}$$

However, before we discuss the explicit barrier crossing result, we present an alternative derivation using the peak-background split approach.

4.1.1 Peak-Background Split

PBS is a heuristic procedure for predicting the large-scale clustering statistics of dark matter halos. All fields are split into long and short modes—i.e. the Gaussian fields in eq. (4.2) are written as $\phi = \phi_s + \phi_\ell$ and $\psi = \psi_s + \psi_\ell$. The short scales ($\lesssim R_M \lesssim 10$ Mpc$/h$) determine halo formation, while the long scales ($\gtrsim 100$ Mpc$/h$) are the ones on which we want to measure the clustering of halos. Long modes are therefore always much larger than the Lagrangian size of the halos that we consider, i.e. $R_M k_\ell \ll 1$. The precise split into long and short modes isn't important for physical observables, as long as it satisfies the above constraints.

The long-wavelength modes alter the statistical properties of the small-scale fluctuations. For instance, to lowest order, the locally measured small-scale power is $\sigma = \bar{\sigma}\,[1 + 2f_{\rm NL}(1+\Pi)\psi_\ell]$, and the locally measured halo number density is

$$n_{\rm h}(\boldsymbol{x}) = \bar{n}_{\rm h}\left(\delta_c - \delta_\ell\,;\bar{\sigma}\,[1 + 2f_{\rm NL}(1+\Pi)\psi_\ell]\right)\ . \tag{4.8}$$

Taylor expanding this expression, we get

$$\delta_{\rm h} \equiv \frac{\delta n_{\rm h}}{\bar{n}_{\rm h}} = b_g\delta_\ell + \beta_f(1+\Pi)f_{\rm NL}\psi_\ell\ \ , \tag{4.9}$$

where

$$b_g \equiv \frac{\partial \ln n_{\rm h}}{\partial \delta_\ell} \quad \text{and} \quad \beta_f \equiv 2\frac{\partial \ln n_{\rm h}}{\partial \ln \sigma}\ . \tag{4.10}$$

Hence, we find

$$P_{\rm mh} = \left(b_g + \beta_f \frac{f_{\rm NL}}{\alpha(k)}\right) P_{\rm mm}\ , \tag{4.11}$$

and

$$P_{\rm hh} = \left(b_g^2 + 2b_g\beta_f\frac{f_{\rm NL}}{\alpha(k)} + \beta_f^2\frac{\left(\frac{5}{6}\right)^2\tau_{\rm NL}}{\alpha^2(k)}\right) P_{\rm mm}\ . \tag{4.12}$$

This leads to large-scale halo stochasticity of the form

$$r = \left(\left(\tfrac{5}{6}\right)^2\tau_{\rm NL} - f_{\rm NL}^2\right)\frac{\beta_f^2}{\alpha^2(k)}\ . \tag{4.13}$$

As $\Pi \to 0$, this reduces to the classic $f_{\rm NL}$ model, with $\tau_{\rm NL} = \left(\frac{6}{5}f_{\rm NL}\right)^2$ and hence no stochasticity.

4.1.2 Barrier Crossing

Next, we show that eq. (4.13) can be reproduced precisely from the barrier crossing analysis of the previous section. In Appendix A, we show that only the lowest-order cumulants will be significant. Here, we calculate the relevant cumulants explicitly: Using eq. (4.5), we get

$$f_{1,2} = f_{\hat{1},2} \ \xrightarrow{k\to 0}\ 4\,\frac{f_{\rm NL}}{\alpha(k)}\ . \tag{4.14}$$

The order-of-magnitude estimates in Appendix A suggest that this will be the dominant contribution. In particular, we expect, $f_{1,2} > f_{1,3}$. We can confirm this explicitly. Using eq. (4.6), we get

$$f_{1,3} = f_{\hat{1},3} \ \xrightarrow{k\to 0}\ 4\,\frac{\left(\frac{5}{6}\right)^2\tau_{\rm NL}}{\alpha(k)}\cdot\kappa_3^{(f_{\rm NL}=1)}\ , \tag{4.15}$$

where

$$\kappa_3^{(f_{\rm NL}=1)}(M) \equiv \frac{6}{\sigma_M^3} \int_{\boldsymbol{q}_1} \int_{\boldsymbol{q}_2} \alpha_M(q_1)\alpha_M(q_2)\alpha_M(q_{12})P_\Phi(q_1)P_\Phi(q_2) \ . \tag{4.16}$$

Since $\kappa_3^{(f_{\rm NL}=1)}$ is of order Δ_Φ, we see that the condition $f_{1,3} \ll f_{1,2}$ is equivalent to $f_{\rm NL}(1+\Pi)\Delta_\Phi \ll 1$. This latter condition is always satisfied if all fields are weakly coupled.[9]

Finally, using eq. (4.7), we get

$$f_{2,2} \xrightarrow{k\to 0} 16\,\frac{\left(\frac{5}{6}\right)^2 \tau_{\rm NL}}{\alpha^2(k)} \ . \tag{4.18}$$

Substituting the above into eq. (3.38) gives

$$r = \left(\left(\tfrac{5}{6}\right)^2 \tau_{\rm NL} - f_{\rm NL}^2\right) \frac{\beta_f^2}{\alpha^2(k)} \ , \tag{4.19}$$

where we have used the relation $\beta_f = 4\beta_2 = 2(\nu_c - 1)$, which can be derived by evaluating the derivative $\beta_f = 2\partial \ln n_{\rm h}/\partial \ln \sigma$ in the barrier crossing model [27]. Comparing with eq. (4.13), we find that barrier crossing and peak-background split give consistent answers.

4.2 $g_{\rm NL}$ Cosmology

As our next example, we consider a cubic form of local non-Gaussianity.[10] In this case, the non-Gaussian potential is parametrized by the expansion

$$\Phi = \phi + g_{\rm NL}\left(\phi^3 - 3\langle\phi^2\rangle\phi\right) \ . \tag{4.20}$$

The power spectrum of the non-Gaussian field is

$$P_\Phi(k) = P_\phi(k) + g_{\rm NL}^2 P_{\phi^3}(k) \ , \tag{4.21}$$

where

$$P_{\phi^3}(k) \equiv 6 \int_{\boldsymbol{q}_1} \int_{\boldsymbol{q}_2} P_\phi(q_1)P_\phi(q_2)P_\phi(|\boldsymbol{k} - \boldsymbol{q}_1 - \boldsymbol{q}_2|) \ . \tag{4.22}$$

We note that for scale-invariant initial conditions, $(k^3/2\pi^2)P_\phi(k) = \Delta_\phi^2$, the power spectrum P_{ϕ^3} is infrared divergent. If the IR divergence is regulated by putting the fields in a finite box with length L, then the power spectrum diverges as

$$P_{\phi^3}(k) \ \sim \ 18\,\Delta_\phi^4 \ln^2(kL) P_\phi(k) \ . \tag{4.23}$$

[9] In more detail, to show that $f_{\rm NL}(1+\Pi)\Delta_\Phi \ll 1$, we argue as follows. Assuming that the field ψ is not strongly coupled, the dimensionless non-Gaussianity parameter $f_{\rm NL}^{(\psi)}\Delta_\psi = f_{\rm NL}(1+\Pi)^{3/2}\Delta_\Phi$ must be $\lesssim 1$. Therefore

$$f_{\rm NL}(1+\Pi)\Delta_\Phi = \Big[f_{\rm NL}\Delta_\Phi\Big]^{1/3} \cdot \Big[f_{\rm NL}(1+\Pi)^{3/2}\Delta_\Phi\Big]^{2/3} \lesssim [10^{-3}]^{1/3} \cdot [1] = 10^{-1} \ , \tag{4.17}$$

where the bound on the first factor is the current observational bound $f_{\rm NL} \lesssim 10^2$.

[10] We should say from the outset that the large-scale stochasticity in the $g_{\rm NL}$ model will be too small to be observationally relevant. Although the non-stochastic and stochastic contributions to $P_{\rm hh}(k)$ will turn out to be parametrically identical ($\sim g_{\rm NL}^2\Delta_\Phi^2 P_\Phi(k)$), the non-stochastic contribution is typically larger by a constant factor $\approx 10^4$. Nevertheless, the $g_{\rm NL}$ example provides an interesting check of our formalism.

On large scales, the matter power spectrum therefore is

$$P_{\rm mm}(k) \simeq \alpha^2(k) P_\Phi(k) = P_g(k) \left(1 + 18\, g_{\rm NL}^2 \Delta_\phi^4 \ln^2(kL)\right) \ , \tag{4.24}$$

where we defined $P_g(k) \equiv \alpha^2(k) P_\phi(k)$. Current observational constraints imply that $|g_{\rm NL}\Delta_\phi^2| \ll 1$. To obtain answers to zeroth or first order in $g_{\rm NL}\Delta_\phi^2$, it suffices to set $P_{\rm mm} \simeq P_g$.

For the barrier crossing analysis, we require the following higher-order correlation functions

$$\xi_\Phi^{(4)[\rm tree]}(\boldsymbol{k}_1, \boldsymbol{k}_2, \boldsymbol{k}_3, \boldsymbol{k}_4) = g_{\rm NL}\big[P_1 P_2 P_3 + 23\,\text{perms.}\big] + \mathcal{O}(g_{\rm NL}^2) \ , \tag{4.25}$$

$$\xi_\Phi^{(4)[\rm loop]}(\boldsymbol{k}_1, \boldsymbol{k}_2, \boldsymbol{k}_3, \boldsymbol{k}_4) = 9\, g_{\rm NL}^2\big[P_1 P_2 P_{\phi^2}(k_{13}) + 11\,\text{perms.}\big] \ , \tag{4.26}$$

$$\xi_\Phi^{(6)}(\boldsymbol{k}_1, \boldsymbol{k}_2, \boldsymbol{k}_3, \boldsymbol{k}_4, \boldsymbol{k}_5, \boldsymbol{k}_6) = 36\, g_{\rm NL}^2\big[P_1 P_2 P_3 P_4 P_{125} + 89\,\text{perms.}\big] \ , \tag{4.27}$$

where $k_{ij} = |\boldsymbol{k}_i + \boldsymbol{k}_j|$, $P_i = P_\phi(k_i)$, $P_{ijk} = P_\phi(|\boldsymbol{k}_i + \boldsymbol{k}_j + \boldsymbol{k}_k|)$, and

$$P_{\phi^2}(k) \equiv 2\int_{\boldsymbol{q}} P_\phi(q) P_\phi(|\boldsymbol{k} - \boldsymbol{q}|) \ \sim \ 4\Delta_\phi^2 \ln(kL) P_\phi(k) \ . \tag{4.28}$$

Note that odd-point correlation functions $\xi_\Phi^{(2N+1)}$ are zero due to the $\Phi \to -\Phi$ symmetry. Next, we will derive the stochastic halo bias both in peak-background split and in barrier crossing.

4.2.1 Peak-Background Split

The PBS analysis proceeds as before. Splitting the Gaussian potential into long and short modes, $\phi = \phi_\ell + \phi_s$, we find that the locally measured small-scale power is $\sigma = \bar\sigma\left[1 + 3g_{\rm NL}\left(\phi_\ell^2 - \langle\phi_\ell^2\rangle\right)\right]$. Moreover, the locally measured value of $f_{\rm NL}$ is $f_{\rm NL}^{\rm eff} = 3g_{\rm NL}\phi_\ell$ [28]. The halo number density therefore is

$$n_{\rm h}(\boldsymbol{x}) = \bar n_{\rm h}\left(\delta_c - \delta_\ell\,; \bar\sigma\left[1 + 3g_{\rm NL}\left(\phi_\ell^2 - \langle\phi_\ell^2\rangle\right)\right]; f_{\rm NL}^{\rm eff}\right) \ , \tag{4.29}$$

where $\delta_\ell \simeq \alpha(k_\ell)\phi_\ell$. Taylor expanding this expression, we find

$$\delta_{\rm h} = b_g\delta_\ell + \tfrac{3}{2}\beta_f g_{\rm NL}\left(\phi_\ell^2 - \langle\phi_\ell^2\rangle\right) + \beta_g g_{\rm NL}\phi_\ell \ , \tag{4.30}$$

where b_g and β_f are the same as in (4.10), and

$$\beta_g \equiv 3\frac{\partial \ln n_{\rm h}}{\partial f_{\rm NL}} \ . \tag{4.31}$$

It follows that

$$P_{\rm mh} = b_g P_{\rm mm} + \beta_g g_{\rm NL} P_{{\rm m}\phi} = \left(b_g + \beta_g \frac{g_{\rm NL}}{\alpha(k)}\right) P_{\rm mm} \ , \tag{4.32}$$

and

$$P_{\rm hh} = \left(b_g + \beta_g \frac{g_{\rm NL}}{\alpha(k)}\right)^2 P_{\rm mm} + \frac{9}{4}\beta_f^2 g_{\rm NL}^2 P_{\phi^2} \ . \tag{4.33}$$

This implies a large-scale halo stochasticity of the form

$$r = \frac{9}{4}\beta_f^2 g_{\rm NL}^2 \frac{P_{\phi^2}}{P_{\rm mm}} \ . \tag{4.34}$$

4.2.2 Barrier Crossing

We now show that the same result is obtained from barrier crossing. In Appendix A, we argue that only the first few cumulants need to be taken into account. It is straightforward to compute them explicitly. From eqs. (4.25) and (4.27), we get

$$f_{1,3}(k) \xrightarrow{k\to 0} \frac{3g_{\rm NL}}{\alpha(k)}\,\kappa_3^{(f_{\rm NL}=1)} \qquad \text{and} \qquad f_{3,3}(k) = [f_{1,3}(k)]^2 \ . \tag{4.35}$$

This only contributes to the non-stochastic bias. However, since $f_{\hat{1},2} = 0$, stochastic bias arises from $f_{2,2}$. First, we note that the tree-level four-point function (4.25) leads to a very small and scale-independent contribution to $f_{2,2}$:

$$f_{2,2}^{[\rm tree]}(k,M,\bar{M}) \xrightarrow{k\to 0} \frac{12\,g_{\rm NL}}{P_{\rm mm}(k)}\left(\frac{1}{\sigma_M^2}\int_{\boldsymbol{q}}\alpha_M^2(q)P_\phi^2(q) + \frac{1}{\sigma_{\bar{M}}^2}\int_{\boldsymbol{q}}\alpha_{\bar{M}}^2(q)P_\phi^2(q)\right) \ . \tag{4.36}$$

Plugging into eq. (3.38) and noting that $\beta_2 = \frac{1}{4}\beta_f$ and $\tilde{\beta}_2 = \frac{1}{2}$, we get a small scale-dependent contribution to the large-scale stochastic bias

$$r_{[\rm tree]} = \frac{3}{2}\frac{g_{\rm NL}}{P_{\rm mm}(k)}\left(\beta_f^2 + 2\beta_f\right)\left(\frac{1}{\sigma_M^2}\int_{\boldsymbol{q}}\alpha_M^2(q)P_\phi^2(q)\right) \ . \tag{4.37}$$

In practice, this contribution to the large-scale stochasticity can't be used as a probe of initial conditions, since a contribution to r with $r \propto 1/k$ (or equivalently a contribution to $P_{\rm hh}(k)$ which approaches a constant as $k \to 0$) is degenerate with other sources of stochasticity such as second-order Gaussian bias. Finally, the one-loop four-point function (4.26) leads to the following contribution to $f_{2,2}$:

$$f_{2,2}^{[\rm loop]}(k) \xrightarrow{k\to 0} 36\,g_{\rm NL}^2\cdot\frac{P_{\phi^2}(k)}{P_{\rm mm}(k)} \ . \tag{4.38}$$

The corresponding stochasticity parameter is

$$r_{[\rm loop]} = \frac{9}{4}\beta_f^2 g_{\rm NL}^2\frac{P_{\phi^2}(k)}{P_{\rm mm}(k)} \propto \frac{1}{k^4} \ , \tag{4.39}$$

in agreement with the PBS predictions (4.34).

4.3 Quasi-Single-Field Inflation

Our last example is quasi-single field inflation (QSFI) [19]. These models involve extra massive scalar degrees of freedom during inflation. In the simplest examples, a single scalar field σ of mass[11] $m^2 \leq \frac{9}{4}H^2$ mixes with the fluctuation of the inflaton[12] $\delta\phi$. The mixing communicates non-Gaussianity from the hidden (isocurvature) sector to the observable (adiabatic) sector. As we now show, it also leads to a significant stochasticity in the halo bias.

[11] We note that extra scalars with masses close to the Hubble scale H are a natural prediction of supersymmetric theories of inflation (see [20] for further discussion).

[12] Recall that $\delta\phi$ in spatially flat gauge is proportional to the curvature perturbation, $\zeta \equiv \frac{H}{\dot{\phi}}\delta\phi$.

4.3.1 Boosted Four-Point Function

Again, we need the squeezed and collapsed limits of the primordial correlation functions[13] [14, 19, 20]:

$$\lim_{k_1\to 0}\xi_\Phi^{(3)}(\boldsymbol{k}_1,\boldsymbol{k}_2,\boldsymbol{k}_3) = 4f_{\rm NL}\left(\frac{k_1}{k_2}\right)^{\Delta} P_1P_2 \ , \tag{4.40}$$

$$\lim_{k_{12}\to 0}\xi_\Phi^{(4)}(\boldsymbol{k}_1,\boldsymbol{k}_2,\boldsymbol{k}_3,\boldsymbol{k}_4) = \ 16\left(\tfrac{5}{6}\right)^2\tau_{\rm NL}\left(\frac{k_{12}^2}{k_1k_3}\right)^{\Delta} P_1P_3P_{12} \ , \tag{4.41}$$

where we defined the parameter

$$\Delta \equiv \frac{3}{2} - \sqrt{\frac{9}{4}-\frac{m^2}{H^2}} \ . \tag{4.42}$$

The non-trivial momentum scaling of eqs. (4.40) and (4.41) is a remarkable signature of extra Hubble mass scalars during inflation [19, 20, 29, 30]. Moreover, if the mixing between σ and ϕ (or ζ) is parametrized by a small dimensionless number $\varepsilon < 1$, then

$$\tau_{\rm NL} \sim \varepsilon^{-2}\left(\tfrac{6}{5}f_{\rm NL}\right)^2 \ > \ \left(\tfrac{6}{5}f_{\rm NL}\right)^2 \ . \tag{4.43}$$

The enhancement of $\tau_{\rm NL}$ arises because the trispectrum is generated by the exchange of the σ-field which is only weakly coupled to ζ. The size of the four-point function $\langle\zeta^4\rangle$ can be estimated from the square of the three-point function $\langle\zeta^2\sigma\rangle$ at horizon crossing,

$$\langle\zeta^4\rangle \sim \langle\zeta^2\sigma\rangle^2 \sim \varepsilon^{-2}\,\frac{\langle\zeta^3\rangle^2}{\langle\zeta^2\rangle} \ . \tag{4.44}$$

The boost of $\tau_{\rm NL}$ is the result of the small correlation between the curvature fluctuation and the massive field, $\varepsilon \ll 1$. The precise dependence of $f_{\rm NL}$ and $\tau_{\rm NL}$ on the fundamental parameters of the QSFI Lagrangian can be found in [14].

4.3.2 Barrier Crossing

In QSFI, the higher-order N-point functions are suppressed by factors of the power spectrum, just as in our previous examples. The dominant contributions to the large-scale structure signal therefore arise from the squeezed limit of the three-point function and the collapsed limit of the four-point function. The relevant cumulants are

$$\kappa_{\hat{1},2}(k) \ \xrightarrow{k\to 0} \ \frac{4f_{\rm NL}}{\hat{\sigma}}(kR_M)^{\Delta}\,\frac{P_{\rm mm}(k)}{\alpha(k)}\,\frac{\Sigma_M^2(\Delta)}{\sigma_M^2} \ , \tag{4.45}$$

and

$$\kappa_{2,2}(k) \ \xrightarrow{k\to 0} \ 16\left(\tfrac{5}{6}\right)^2\tau_{\rm NL}(k^2R_MR_{\bar{M}})^{\Delta}\,\frac{P_{\rm mm}(k)}{\alpha^2(k)}\,\frac{\Sigma_M^2(\Delta)}{\sigma_M^2}\,\frac{\Sigma_{\bar{M}}^2(\Delta)}{\sigma_{\bar{M}}^2} \ . \tag{4.46}$$

Here, we have defined

$$\Sigma_M^2(\Delta) \equiv \int\frac{{\rm d}^3k_s}{(2\pi)^3}\,W_M^2(k_s)(k_sR_M)^{-\Delta}P_{\rm mm}(k_s) \ , \tag{4.47}$$

[13] See [20] for an intuitive explanation of the scalings in eqs. (4.40) and (4.41).

where the integration variable, k_s, is one of the short momenta and R_M is the smoothing scale defined by eq. (3.4). By definition, $\Sigma_M(0) = \sigma_M$. In the limit $\Delta \to 0$, we recover the results of the $\tau_{\rm NL}$ model. Therefore, we find

$$f_{\hat{1},2} = 4 f_{\rm NL} \frac{(kR_M)^\Delta}{\alpha(k)} \frac{\Sigma_M^2(\Delta)}{\sigma_M^2} \qquad \text{and} \qquad f_{2,2} = \frac{\tau_{\rm NL}}{(\frac{6}{5} f_{\rm NL})^2} f_{\hat{1},2}(M) f_{\hat{1},2}(\bar{M}) \ . \tag{4.48}$$

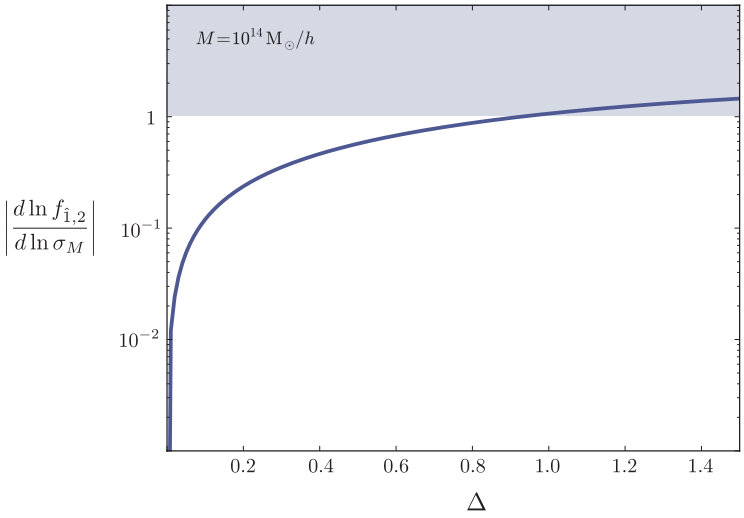

Figure 2: *Numerical evaluation of eqs. (4.47) and (4.48). For $\Delta \gtrsim 1.0$, the cumulant $f_{\hat{1},2}$ depends significantly on the halo mass scale M. This is in contrast to local non-Gaussianity, which corresponds to the limit $\Delta \to 0$.*

To obtain the large-scale stochasticity, we substitute the cumulants into eq. (3.38),

$$r \ = \ \left(\beta_2 + \tilde{\beta}_2 \frac{\partial}{\partial \ln \sigma_M}\right)\left(\beta_2 + \tilde{\beta}_2 \frac{\partial}{\partial \ln \sigma_{\bar{M}}}\right) f_{2,2} \ - \ \left[\left(\beta_2 + \tilde{\beta}_2 \frac{\partial}{\partial \ln \sigma_M}\right) f_{\hat{1},2}\right]^2 \ . \tag{4.49}$$

Because the cumulants depend explicitly on R_M, we have to be concerned that the derivatives with respect to σ_M may this time not be negligible. Indeed, numerical evaluation of the integral shows significant σ_M dependence of $f_{\hat{1},2}$ (see fig. 2). Keeping the derivative terms, we get

$$\begin{aligned} r \ &= \ \left(\left(\tfrac{5}{6}\right)^2 \tau_{\rm NL} - f_{\rm NL}^2\right) \frac{k^{2\Delta}}{\alpha^2(k)} \left[\left(\beta_f + 2\,\frac{d}{d\ln\sigma_M}\right) \frac{R_M^\Delta\, \Sigma_M^2(\Delta)}{\sigma_M^2}\right]^2 \\ &\propto \ \frac{\left(\frac{5}{6}\right)^2 \tau_{\rm NL} - f_{\rm NL}^2}{k^{4-2\Delta}} \ . \end{aligned} \tag{4.50}$$

The characteristic momentum scaling of eq. (4.50) and the natural boost of $\tau_{\rm NL}$ makes halo stochasticity an interesting probe of quasi-single-field inflation.

5 Conclusions

What was the number of light degrees of freedom during inflation? And, what were their interactions? The great virtue of primordial non-Gaussianity is that it is sensitive to these basic questions about the physics of inflation. In particular, it is well-known that the squeezed limit of the primordial three-point function,

$$\lim_{k_1\to 0}\langle \Phi_{\boldsymbol{k}_1}\Phi_{\boldsymbol{k}_2}\Phi_{\boldsymbol{k}_3}\rangle \ , \tag{5.1}$$

can only be large if more than one light field was dynamically relevant during inflation [31, 32]. Remarkably, this statement is independent of the details of the Lagrangian for the inflaton field and its initial conditions. Measurements of the squeezed limit therefore have the potential to rule out all models of single-field inflation [31, 32]. Moreover, the precise scaling in the squeezed limit is sensitive to the details of the mass spectrum [14, 19], allowing a test of extra Hubble mass fields, such as those generically expected in supersymmetric theories [20]. Having a large three-point function in the squeezed limit modulates the two-point function of halos and therefore leads to scale-dependent bias [7]. In the future, this effect may well be our most sensitive probe of the squeezed limit.

In this paper, we have discussed a *stochastic* form of scale-dependent halo bias. This effect arises if the collapsed limit of the primordial four-point function,

$$\lim_{k_{12}\to 0}\langle \Phi_{\boldsymbol{k}_1}\Phi_{\boldsymbol{k}_2}\Phi_{\boldsymbol{k}_3}\Phi_{\boldsymbol{k}_4}\rangle_{\rm c} \ , \tag{5.2}$$

is larger than the square of the squeezed limit of the three-point function. More generally, stochastic bias arises whenever a suitable collapsed limit of an $(M+N)$-point function is larger than the product of the associated squeezed $(M+1)$-point and $(N+1)$-point functions, where $M, N \geq 2$. The key tool for obtaining this result, and a main result of this paper, is a pair of formulas, eqs. (3.26) and (3.36), for the matter-halo and halo-halo power spectra in a general non-Gaussian model parametrized by the N-point functions of the primordial potential.

In non-Gaussian models which generate significant stochastic halo bias, the results of this paper are important even at a qualitative level. As a concrete example, it should be possible to measure $f_{\rm NL}$ and $\tau_{\rm NL}$ independently using stochastic bias. This can be done either by measuring multiple tracer populations and directly estimating large-scale stochasticity (which has the advantage of eliminating sample variance), or from a single tracer population by measuring $P_{\rm hh}(k)$ and using the functional form

$$P_{\rm hh}(k) = b_g^2\left(1 + f_{\rm NL}\frac{2\delta_c}{\alpha(k)} + \tau_{\rm NL}\frac{(\frac{5}{6})^2\delta_c^2}{\alpha^2(k)}\right) \tag{5.3}$$

to fit for b_g, $f_{\rm NL}$ and $\tau_{\rm NL}$ independently. Recently, ref. [36] showed that if only non-stochastic bias is considered, the leading contribution from $\tau_{\rm NL}$ is small (in our language, this corresponds to the $\mathcal{O}(\tau_{\rm NL})$ contribution to $\kappa_{1,3}$) and it is difficult to separate $f_{\rm NL}$ and $\tau_{\rm NL}$, so stochastic bias has an important qualitative effect. As another example, in quasi-single field inflation, the stochastic bias is larger than the non-stochastic bias by a large factor (parametrically ε^{-2}), leading to a similarly large enhancement in signal-to-noise when stochastic bias is considered. We defer quantitative forecasts incorporating stochastic bias for future work.

In general, there is no stochastic bias if only a single field (which may or may not be the inflaton) generates the primordial curvature perturbation and its non-Gaussianity [16]. Measuring stochastic halo bias would therefore teach us about the effective number of degrees of freedom that generated the primordial fluctuations and its higher-order correlations. In particular, stochasticity is sensitive to what we may call "hidden sector non-Gaussianity", i.e. situations in which two fields generate the curvature perturbation, but only one (hidden) field is responsible for its non-Gaussianity. In this paper, we have derived this effect for general non-Gaussian initial conditions. We have also applied our formalism to a number of explicit examples, such as curvaton models [18] and quasi-single field inflation [19]. We have shown that halo bias, in principle, gives us information about the soft limits of both the primordial three-point function and the four-point function. It is therefore a valuable tool in the quest to uncover the physics that created the initial perturbations.

Acknowledgments

We thank Valentin Assassi, Eugene Lim, Marilena LoVerde, Marcel Schmittfull, David Spergel and Matias Zaldarriaga for helpful discussions. D.B. gratefully acknowledges support from a Starting Grant of the European Research Council (ERC STG grant 279617). S.F. acknowledges support from a fellowship at the Department of Astrophysical Sciences of Princeton University. The research of D.G. is supported by the DOE under grant number DE-FG02-90ER40542 and the Martin A. and Helen Chooljian Membership at the Institute for Advanced Study. K.M.S. was supported by a Lyman Spitzer fellowship in the Department of Astrophysical Sciences at Princeton University. Research at Perimeter Institute is supported by the Government of Canada through Industry Canada and by the Province of Ontario through the Ministry of Research & Innovation.

A Convergence of the Edgeworth Expansion

In this appendix, we discuss the convergence properties of the Edgeworth expansion for local non-Gaussianity. In particular, we will estimate the relative size of the cumulants $\kappa_{n,m}(k, M)$ for general n and $m > 0$ in the large-scale limit $k \to 0$. For further discussion see e.g. [33–35]. The results in this appendix are used in the main text in several places: to justify the approximation that non-linear terms in the Edgeworth expansion are negligible in eqs. (3.23) and (3.33), and to justify keeping only certain cumulants in the $\tau_{\rm NL}$ model (§4.1.2) and the $g_{\rm NL}$ model (§4.2.2).

A.1 $\tau_{\rm NL}$ Cosmology

We first consider the $\tau_{\rm NL}$ model of §4.1.

Linear terms.—The leading contribution in the $k \to 0$ limit arises from the following contribution to the connected correlation function

$$\kappa_{n,m} \simeq \mathcal{A}_{n,m} \int \langle \overbrace{\psi_1(\psi\psi)_2}\cdots \overbrace{(\psi\psi)_n \mid (\psi\psi)_{n+1}}\cdots \overbrace{(\psi\psi)_{n+m-1}\psi_{n+m}}\rangle_{\rm c}' \, {\rm d}\mathbf{K} \,, \tag{A.1}$$

where ${\rm d}\mathbf{K} \equiv \prod_i \frac{{\rm d}^3\boldsymbol{k}_i}{(2\pi)^3}\,\alpha_{\scriptscriptstyle M}(k_i)$ and $(\psi\psi)_i$ denotes an auto-convolution evaluated at $\boldsymbol{k}_i$. The prime on the correlation function denotes that we have dropped an overall momentum conserving delta-function. The amplitude of the cumulant is given by

$$\mathcal{A}_{n,m} \equiv c_{n,m}(1+\Pi)^{2(n+m-2)} f_{\rm NL}^{n+m-2} \,, \qquad \text{where} \qquad c_{n,m} \equiv \frac{n!m!\,2^{n+m-2}}{\sigma_{\scriptscriptstyle M}^n \sigma_{\scriptscriptstyle \bar{M}}^m} \,. \tag{A.2}$$

We arrived at eq. (A.1) by using the definition of Φ in eq. (4.2) and expanding out terms to produce a connected correlation function. The numerical factor $c_{n,m}$ in the amplitude (A.2) arises from the sum over equivalent contractions of the fields. The vertical line in (A.1) separates the first n terms from the last m. Each contraction gives a factor of P_ψ, and the contraction crossing the vertical line carries momentum k, giving a factor of $P_\psi(k)$ that can be taken out of the integral. The power spectrum $P_\psi(k)$ diverges as $k \to 0$ and gives the largest[14] contribution to $\kappa_{n,m}$. The remaining integral over ${\rm d}\mathbf{K}$ will typically be dominated by the non-linear scale $k_{\rm nl}$, where $k_{\rm nl}^3 P_{\rm mm}(k_{\rm nl}) \sim \alpha_{\scriptscriptstyle M}^2(k_{\rm nl})\Delta_\Phi^2 \sim 1$. Therefore, we may estimate the integral using $\alpha_{\scriptscriptstyle M} \sim \Delta_\Phi^{-1}$, to get

$$\kappa_{1,m} \;\simeq\; c_{1,m}\,(1+\Pi)^{m-2}\; f_{\rm NL}^{m-1}\;\Delta_\Phi^{m-2}\cdot\frac{P_{\rm mm}(k)}{\alpha(k)} \qquad \text{for} \;\; m>1 \,, \tag{A.3}$$

$$\kappa_{n,m} \;\simeq\; c_{n,m}\,(1+\Pi)^{n+m-3}\; f_{\rm NL}^{n+m-2}\;\Delta_\Phi^{n+m-4}\cdot\frac{P_{\rm mm}(k)}{\alpha^2(k)} \qquad \text{for} \;\; n \text{ and } m>1 \,. \tag{A.4}$$

The factor $n!m!$ appearing in $c_{n,m}$ is canceled explicitly in the Edgeworth expansion (3.13), and as shown in §4.1.2, the condition $f_{\rm NL}(1+\Pi)\Delta_\Phi \ll 1$ is always satisfied. This implies that higher-order cumulants are subdominant relative to lower-order ones, and hence the only terms we have to keep in the $\tau_{\rm NL}$ model are $\kappa_{1,1}$, $\kappa_{1,2} = \kappa_{2,1}$ and $\kappa_{2,2}$.

[14] Subleading contributions arise when both linear ψ terms appear on the same side. In such cases, two contractions cross the vertical line, and the resulting cumulant is finite in the $k \to 0$ limit.

Non-linear terms.—When expanding the exponential in the Edgeworth expansion (3.13) we also encounter non-linear terms such as $\kappa^P_{n,m}(\boldsymbol{x})$. First, we will show that, for n and/or $m > 1$, these terms are suppressed by the near-Gaussianity of the primordial perturbations. We distinguish two cases:

- When $n > 1$ and $m > 1$, we take powers of the contributions in (A.4), to find

$$\kappa^P_{n,m} \;\sim\; \Big[c_{n,m}\,(1+\Pi)^{n+m-3}\,f_{\rm NL}^{n+m-2}\,\Delta_\Phi^{n+m-4}\Big]^P \cdot \frac{P_{\rm mm}(k)}{\alpha^2(k)} \cdot \Delta_\Phi^{2(P-1)}\ln^{P-1}(kL)\;, \quad \text{(A.5)}$$

  where L is an infrared cutoff. This can be written as

$$\kappa^P_{n,m} \;\sim\; \kappa_{n,m}\cdot c^P_{n,m}\big[f_{\rm NL}(1+\Pi)\Delta_\Phi\big]^{(P-1)(n+m-2)}(1+\Pi)^{-P}\ln^{P-1}(kL)\;. \quad \text{(A.6)}$$

  Using $f_{\rm NL}(1+\Pi)\Delta_\Phi \ll 1$ and $(1+\Pi) > 1$, we see that $\kappa^P_{n,m}$ is suppressed relative to $\kappa_{n,m}$ for $n, m > 1$.

- When $n = 1$ and $m > 1$, the situation is slightly different. If we take higher powers of the results in (A.3), we find for $P > 1$,

$$\begin{aligned}\kappa^P_{1,m} \;&\sim\; c^P_{1,m}\left[(1+\Pi)^{m-2}\,f_{\rm NL}^{m-1}\,\Delta_\Phi^{m-2}\right]^P\Delta_\Phi^{P-1}P_{\rm mm}(k_{\rm nl})\\ &\sim\; \kappa_{1,m}\cdot c^{P-1}_{1,m}\big[f_{\rm NL}(1+\Pi)\Delta_\Phi\big]^{(P-1)(m-1)}(1+\Pi)^{-P}\alpha(k)\cdot\frac{P_{\rm mm}(k_{\rm nl})}{P_{\rm mm}(k)}\;. \end{aligned}\quad \text{(A.7)}$$

  Again, as we increase the power P, the contribution is suppressed. However, there is a clear difference between $P = 1$ and $P > 1$. Nevertheless, in the limit $k \to 0$, $[P_{\rm mm}(k)/\alpha(k)]^{-1} \propto k$ so that these contributions vanish relative to $\kappa_{1,m}$.

Next, we consider products of the Gaussian piece, $\kappa^P_{1,1}$. We find for $P > 1$,

$$\begin{aligned}\kappa^P_{1,1} \;&\sim\; P^P_{\rm mm}(k_{\rm eq})\cdot(k_{\rm eq})^{3P-3}\\ &\sim\; \kappa_{1,1}\,\frac{P_{\rm mm}(k_{\rm eq})}{P_{\rm mm}(k)}\,\Delta^{P-1}_{\rm m}(k_{\rm eq})\;. \end{aligned}\quad \text{(A.8)}$$

Here, $\kappa_{1,1}$ receives its largest contribution from the peak of the linear matter power spectrum $\Delta^2_{\rm m}(k) = k^3\hat{P}_{\rm m}(k)$ which occurs at $k = k_{\rm eq}$, the scale set by matter-radiation equality. Because $\Delta_{\rm m}(k_{\rm eq}) < 1$ at that scale, the modes are still linear and higher powers of $\kappa_{1,1}$ will be suppressed. However, in the limit $k \to 0$, $\kappa_{1,1}$ vanishes, while $\kappa^P_{1,1}$ is finite for $P > 1$. This gives a small constant contribution to the halo power spectrum $P_{\rm hh}$ which is a free parameter in practice (we discussed this in the context of the $g_{\rm NL}$ model in §4.2.2).

Finally, we look at terms of the form $\kappa^P_{n,m}\kappa^Q_{n',m'}$. We may bound these contributions by using the above estimates with the convolution $\kappa^P_{n,m}\star\kappa^Q_{n',m'} = \int_{\boldsymbol{q}}\kappa^P_{m,n}(|\boldsymbol{q}|)\kappa^Q_{n',m'}(|\boldsymbol{k}-\boldsymbol{q}|)$. For $n, m > 1$, the convolution will be dominated by the IR, and we find

$$\kappa^P_{n,m}\star\kappa^Q_{n',m'} \;\sim\; \kappa^P_{n,m}(k)\kappa^Q_{n',m'}(k)\,\frac{\alpha^2(k)\ln(kL)}{P_{\rm mm}(k)}\;. \quad \text{(A.9)}$$

For $m = m' = 1$, the convolution is dominated by physics at the non-linear scale, so we may simply multiply (A.7) and/or (A.8) to find

$$\kappa^P_{n,1}\star\kappa^Q_{n',1} \;\sim\; \kappa^P_{n,1}(k)\kappa^Q_{n',1}(k)\,k^3_{\rm nl}\;. \quad \text{(A.10)}$$

As a result, convolutions of different cumulants will be suppressed by $f_{\rm NL}(1+\Pi)\Delta_\Phi \ll 1$.

A.2 $g_{\rm NL}$ Cosmology

Similar arguments apply to the $g_{\rm NL}$ model of §4.2.

Linear terms.—First, we note that $\kappa_{n,m} = 0$, unless $n+m$ is even. Moreover, only for both n and m odd do we get a scale-dependent tree-level contribution to the cumulant. (In the main text, we discuss the important special case $\kappa_{2,2}$.) Schematically, we can write $\kappa_{n,m} \sim g_{\rm NL}^{\beta}\,\Delta_\Phi^{\gamma}$. At tree level, we then find

$$\kappa_{1,m} \sim g_{\rm NL}^{\frac{m-1}{2}}\,\Delta_\Phi^{m-2}\cdot\frac{P_{\rm mm}(k)}{\alpha(k)} \qquad \text{for } \; m \text{ odd}\,, \tag{A.11}$$

$$\kappa_{n,m} \sim g_{\rm NL}^{\frac{n+m}{2}-1}\,\Delta_\Phi^{m+n-4}\cdot\frac{P_{\rm mm}(k)}{\alpha^2(k)} \qquad \text{for } \; n,m \text{ odd and } >1\,. \tag{A.12}$$

Since current observational constraints imply $|g_{\rm NL}\Delta_\Phi^2| \ll 1$, the only tree-level terms that we need to keep are $\kappa_{1,1}$, $\kappa_{1,3}=\kappa_{3,1}$ and $\kappa_{3,3}$. As we discuss in the main text, there is also an interesting loop contribution to $\kappa_{2,2}$.

Non-linear terms.—As in the $\tau_{\rm NL}$ model, products of cumulants of the form $\kappa^P_{n,m}$ will be suppressed due to the near-Gaussianity of the perturbations. The contributions of higher powers of $\kappa_{n,m}$ is nearly identical in both cases:

- When $n>1$ and $m>1$, we take powers of the contributions in (A.12), to find

$$\begin{aligned}\kappa^P_{n,m} \;&\sim\; \Big[\,g_{\rm NL}^{\frac{n+m}{2}-1}\Delta_\Phi^{m+n-4}\,\Big]^P\cdot\frac{P_{\rm mm}(k)}{\alpha^2(k)}\cdot\Delta_\Phi^{2(P-1)}\ln^{P-1}(kL)\\ &\sim\; \kappa_{n,m}\Big[\,g_{\rm NL}\Delta_\Phi^2\,\Big]^{(P-1)(\frac{n+m-2}{2})}\ln^{P-1}(kL)\,.\end{aligned} \tag{A.13}$$

  Clearly, if $g_{\rm NL}\Delta_\Phi^2 \ll 1$, then the higher powers of $\kappa_{n,m}$ are suppressed (if we assume that the log is small).

- When $n=1$ and $m>1$, we take higher powers of the results in (A.11), to find for $P>1$

$$\begin{aligned}\kappa^P_{1,m} \;&\sim\; \Big[\,g_{\rm NL}^{\frac{m-1}{2}}\Delta_\Phi^{m-2}\Big]^P\,\Delta_\Phi^{P-1}P_{\rm mm}(k_{\rm nl})\\ &\sim\; \kappa_{1,m}\left[g_{\rm NL}\Delta_\Phi^2\right]^{(P-1)(\frac{m-1}{2})}\alpha(k)\cdot\frac{P_{\rm mm}(k_{\rm nl})}{P_{\rm mm}(k)}\,.\end{aligned} \tag{A.14}$$

  Again, we find that $P>1$ contributions are suppressed by powers of $g_{\rm NL}\Delta_\Phi^2 \ll 1$. As in the $\tau_{\rm NL}$ model, we find that $P=1$ has a different scaling with k from $P>1$.

It should be clear that other cumulants behave in the same way as in the $\tau_{\rm NL}$ model and will be suppressed by factors of $g_{\rm NL}\Delta_\Phi^2$.

References

[1] S. Ferraro, K. Smith, D. Green, and D. Baumann, "On the Equivalence of Barrier Crossing, Peak-Background Split, and Local Biasing", *to appear*.

[2] A. Guth, "The Inflationary Universe: A Possible Solution To The Horizon And Flatness Problems," Phys. Rev. D **23**, 347 (1981); • A. Linde, "A New Inflationary Universe Scenario: A Possible Solution Of The Horizon, Flatness, Homogeneity, Isotropy And Primordial Monopole Problems," Phys. Lett. B **108**, 389 (1982); • A. Albrecht and P. Steinhardt, "Cosmology For Grand Unified Theories With Radiatively Induced Symmetry Breaking," Phys. Rev. Lett. **48**, 1220 (1982); • for a review see D. Baumann, "TASI Lectures on Inflation," [arXiv:0907.5424 [hep-th]].

[3] E. Komatsu et al., "Non-Gaussianity as a Probe of the Physics of the Primordial Universe and the Astrophysics of the Low Redshift Universe," arXiv:0902.4759 [astro-ph.CO].

[4] E. Komatsu, "Hunting for Primordial Non-Gaussianity in the Cosmic Microwave Background," Class. Quant. Grav. **27**, 124010 (2010).

[5] V. Desjacques and U. Seljak, "Primordial Non-Gaussianity in the Large-Scale Structure of the Universe," [arXiv:1006.4763 [astro-ph.CO]].

[6] M. Liguori, E. Sefusatti, J. Fergusson, and E. P. S. Shellard, "Primordial Non-Gaussianity and Bispectrum Measurements in the Cosmic Microwave Background and Large-Scale Structure," Adv. Astron. **2010**, 980523 (2010).

[7] N. Dalal, O. Dore, D. Huterer, and A. Shirokov, "The Imprints of Primordial Non-Gaussianities on Large-Scale Structure: Scale-Dependent Bias and Abundance of Virialized Objects," Phys. Rev. **D77**, 123514 (2008).

[8] S. Matarrese and L. Verde, "The Effect of Primordial Non-Gaussianity on Halo Bias," Astrophys. J. **677**, L77 (2008).

[9] C. Byrnes, M. Sasaki, and D. Wands, "The Primordial Trispectrum from Inflation," Phys. Rev. D **74**, 123519 (2006).

[10] T. Suyama and M. Yamaguchi, "Non-Gaussianity in the Modulated Reheating Scenario," Phys. Rev. D **77**, 023505 (2008).

[11] N. Sugiyama, E. Komatsu, and T. Futamase, "Non-Gaussianity Consistency Relation for Multi-Field Inflation," Phys. Rev. Lett. **106**, 251301 (2011).

[12] A. Lewis, 'The Real Shape of Non-Gaussianities," JCAP **1110**, 026 (2011).

[13] K. Smith, M. LoVerde, and M. Zaldarriaga, "A Universal Bound on N-point Correlations from Inflation," Phys. Rev. Lett. **107**, 191301 (2011).

[14] V. Assassi, D. Baumann, and D. Green, "On Soft Limits of Inflationary Correlation Functions," arXiv:1204.4207 [hep-th].

[15] A. Kehagias and A. Riotto, "Operator Product Expansion of Inflationary Correlators and Conformal Symmetry of de Sitter," arXiv:1205.1523 [hep-th].

[16] T. Suyama, T. Takahashi, M. Yamaguchi, and S. Yokoyama, "On Classification of Models of Large Local-Type Non-Gaussianity," JCAP **1012**, 030 (2010).

[17] C. Byrnes, S. Nurmi, G. Tasinato, and D. Wands, "Inhomogeneous Non-Gaussianity," JCAP **1203** (2012) 012.

[18] D. Tseliakhovich, C. Hirata, and A. Slosar, "Non-Gaussianity and Large-Scale Structure in a

Two-Field Inflationary Model," Phys. Rev. **D82**, 043531 (2010).

[19] X. Chen and Y. Wang, "Quasi-Single-Field Inflation and Non-Gaussianities," JCAP **1004**, 027 (2010).

[20] D. Baumann and D. Green, "Signatures of Supersymmetry from the Early Universe," Phys. Rev. D **85**, 103520 (2012).

[21] W. Press and P. Schechter, "Formation of Galaxies and Clusters of Galaxies by Self-Similar Gravitational Condensation," Astrophys. J. **187**, 425 (1974).

[22] F. Bernardeau, S. Colombi, E. Gaztanaga, and R. Scoccimarro, "Large-Scale Structure of the Universe and Cosmological Perturbation Theory," Phys. Rept. **367**, 1 (2002).

[23] M. Grossi, L. Verde, C. Carbone, K. Dolag, E. Branchini, F. Iannuzzi, S. Matarrese, and L. Moscardini, "Large-Scale Non-Gaussian Mass Function and Halo Bias: Tests on N-body Simulations," Mon. Not. Roy. Astron. Soc. **398**, 321 (2009).

[24] N. Hamaus, U. Seljak, V. Desjacques, R. Smith, and T. Baldauf, "Minimizing the Stochasticity of Halos in Large-Scale Structure Surveys," Phys. Rev. D **82**, 043515 (2010).

[25] K. Smith and M. LoVerde, "Local Stochastic Non-Gaussianity and N-body Simulations," JCAP **1111**, 009 (2011).

[26] V. Desjacques, D. Jeong, and F. Schmidt, "Non-Gaussian Halo Bias Re-examined: Mass-Dependent Amplitude from the Peak-Background Split and Thresholding," Phys. Rev. D **84**, 063512 (2011).

[27] A. Slosar, C. Hirata, U. Seljak, S. Ho, and N. Padmanabhan, "Constraints on Local Primordial Non-Gaussianity from Large-Scale Structure," JCAP **0808**, 031 (2008).

[28] K. Smith, S. Ferraro, and M. LoVerde, "Halo Clustering and $g_{\rm NL}$-type Primordial non-Gaussianity," JCAP **1203**, 032 (2012).

[29] E. Sefusatti, J. Fergusson, X. Chen, and E. P. S. Shellard, "Effects and Detectability of Quasi-Single Field Inflation in the Large-Scale Structure and Cosmic Microwave Background," arXiv:1204.6318 [astro-ph.CO].

[30] J. Norena, L. Verde, G. Barenboim, and C. Bosch, "Prospects for Constraining the Shape of Non-Gaussianity with the Scale-Dependent Bias," arXiv:1204.6324 [astro-ph.CO].

[31] J. Maldacena, "Non-Gaussian Features of Primordial Fluctuations in Single-Field Inflationary Models," JHEP **0305**, 013 (2003).

[32] P. Creminelli and M. Zaldarriaga, "Single-Field Consistency Relation for the Three-Point Function," JCAP **0410**, 006 (2004).

[33] M. LoVerde, A. Miller, S. Shandera, and L. Verde, "Effects of Scale-Dependent Non-Gaussianity on Cosmological Structures," JCAP **0804**, 014 (2008).

[34] S. Shandera, "The Structure of Correlation Functions in Single-Field Inflation," Phys. Rev. D **79**, 123518 (2009).

[35] N. Barnaby and S. Shandera, "Feeding your Inflaton: Non-Gaussian Signatures of Interaction Structure," JCAP **1201**, 034 (2012).

[36] M. Biagetti, V. Desjacques, and A. Riotto, "Testing Multi-Field Inflation with Galaxy Bias," arXiv:1208.1616 [astro-ph.CO].